Yang-Rice-Zhang description of checkerboard pattern and autocorrelation of photoemission data in high-temperature superconductors

E. Bascones* and B. Valenzuela†
Instituto de Ciencia de Materiales de Madrid, CSIC, Cantoblanco, E-28049 Madrid, Spain
(Received 19 September 2007; revised manuscript received 16 November 2007; published 31 January 2008)

In the pseudogap state, the spectrum of the autocorrelation of angle resolved photoemission spectroscopy (AC-ARPES) data of $Bi_2Sr_2CaCu_2O_{8+\delta}$ presents nondispersive peaks in momentum space, while dispersive peaks are found in the superconducting state. Both dispersive and nondispersive features compare well with those found in Fourier transform scanning tunneling spectroscopy (FT-STS). Here, we show that the experimental AC-ARPES spectrum can be reproduced using the Yang-Rice-Zhang model for the pseudogap with no intrinsic charge ordering or symmetry breaking. This result suggests that quantum interference of quasiparticles can also play a role in the nondispersive features of FT-STS associated with the so-called checkerboard pattern in the pseudogap state. Due to the competition of superconductivity and pseudogap included in this model, we obtain both dispersive and nondispersive peaks in the AC-ARPES data of superconducting underdoped cuprates.

DOI: 10.1103/PhysRevB.77.024527 PACS number(s): 74.72.−h, 74.20.Mn, 74.25.Jb

I. INTRODUCTION

In the pseudogap (PG) state of underdoped cuprates instead of a complete Fermi surface,[1] just a Fermi arc around the nodal (diagonal) direction is seen, while the antinodal region close to $(\pi,0)$ is gapped. There are two main proposals to describe the PG state, which is believed to be the key in understanding the superconductivity in of these materials. In one of them, the PG and the superconductivity compete, while in the other one, the PG is the precursor of superconductivity. The competing scenario has found further support[2] with recent Raman[3] and photoemission[4–7] experiments which have shown that the nodal-antinodal dichotomy persists in the superconducting (SC) state in the form of two different energy scales in nodal and antinodal regions. The nature of the possible competing state remains controversial.[2,8] Most of the proposals[8] involve charge ordering and/or breaking of the symmetry. To date, there is no accepted evidence of such symmetry breaking.

Strong support for intrinsic charge-ordering models came from the observation of the so-called checkerboard pattern in Fourier transform scanning tunneling spectroscopy (FT-STS) measurements.[9–18] Fourier transform scanning tunneling spectroscopy (FT-STS) gives information on the momentum $\mathbf{q}$ and energy ω dependent density of states $n(\mathbf{q},\omega)$. The checkerboard pattern refers to the peaks in $n(\mathbf{q},\omega)$ found at $\mathbf{q}\sim(\pm 2\pi/\lambda,0)$ and $(0,\pm 2\pi/\lambda)$, with $\lambda\sim 4-5$ measured in units of the lattice spacing. The checkerboard peaks are nondispersive, i.e., their position in momentum space does not change with energy. Together with this modulation, weaker substructure at $\mathbf{q}\sim[\pm 3(2\pi)/4,0]$ and $[0,\pm 3(2\pi)/4]$ has been detected.[13–17]

The lack of dispersion of the checkerboard peaks differentiates them from another kind of peaks also found by FT-STS in the superconducting state, which disperse with binding energy. It is generally accepted that these dispersive features are a consequence of quantum interference of quasiparticles by elastic scattering[19–21] though a quantitative understanding using the full machinery of T matrix is still lacking.[21] In this picture, the modulation of the density of states is induced by disorder. In its most simple description, maxima in $n(\mathbf{q},\omega)$ are expected at those momenta which connect the states with the largest joint density of states (JDOS).

On the other hand, the origin of the checkerboard remains controversial and highly debated. Proposals based on the JDOS picture have been discussed.[22,23] However, due to its nondispersive nature,[22] most of the models for the checkerboard involve states intrinsically inhomogeneous and charge ordering.[13,24–33]

The JDOS is related to the spectral function by

$$JDOS(\mathbf{q},\omega)=\sum_k A(\mathbf{k},\omega)A(\mathbf{k}+\mathbf{q},\omega). \quad (1)$$

Forgetting about matrix element and resolution effects, the spectral function is measured by angle resolved photoemission spectroscopy (ARPES). The JDOS can thus be obtained experimentally from the autocorrelation of ARPES (AC-ARPES) data.[34] The influence of matrix element effects can be further checked by changing the polarization of the light used.[35] The AC-ARPES spectrum of $Bi_2Sr_2CaCu_2O_{8+\delta}$ (Bi2212) in the superconducting state[35,36] shows dispersive peaks in good agreement with those found in FT-STS. In the pseudogap state, AC-ARPES data present[36] peaks near $(0.4\pi,0)$ and $(1.4\pi,0)$ with very little dispersion, in contrast to the ones in the superconducting state. The $(0.4\pi,0)$ nondispersive peaks compare well with those responsible for the checkerboard in FT-STS. Based on these results, it has been suggested[36] that all peaks in both the superconducting state and the pseudogap state have a common origin in AC-ARPES and in FT-STS. A theoretical model which presents such nondispersive behavior in the JDOS in the pseudogap is still lacking.

In this paper, we study the AC-ARPES spectrum using the model recently proposed by Yang, Rice, and Zhang (YRZ) for the pseudogap.[37] In agreement with the experimental results, we find peaks with very little dispersion (referred as

nondispersive in the following) in the pseudogap, while clearly dispersive peaks appear in the superconducting state. Neither intrinsic charge ordering or symmetry breaking is involved in this model or in the explanation of the experimental results. The different behaviors in the PG and SC states are related to the different evolutions of the constant energy contour size with binding energy and the existence of Fermi arcs at zero energy in the PG. Furthermore, we show that both dispersive and nondispersive peaks can be present at low doping x in the superconducting state, and we relate this result to the U shape of the SC gap found in ARPES in underdoped superconducting cuprates.[2,4,5] The dispersive ones are restricted to low energies, lower with underdoping. The nondispersive features in the superconducting state can dominate the spectrum in cuprates in low T_c cuprates at small doping and are a consequence of the persistence of pseudogap correlations below T_c and their imprint on the spectral function and dispersion. We argue that our predictions for the position and dispersion of the peaks in AC-ARPES can be extended to the tunneling experiments.

II. MODEL

The YRZ model[37] assumes that the pseudogap can be described as a doped spin liquid and proposes a phenomenological Green's function to characterize it.

$$G_{PG}^{YRZ}(\mathbf{k},\omega) = \frac{g_t}{\omega - \xi(\mathbf{k}) - \Sigma_R(\mathbf{k},\omega)} + G_{inc}. \tag{2}$$

Here, $\xi(\mathbf{k}) = \epsilon_0(\mathbf{k}) - 4t'(x)\cos k_x \cos k_y - 2t''(x)(\cos 2k_x + \cos 2k_y) - \mu_p$, $\epsilon_0(\mathbf{k}) = -2t(x)(\cos k_x + \cos k_y)$, and μ_p is determined from the Luttinger sum rule. Moreover, g_t is a Gutzwiller spectral weight factor and the band parameters $t(x)$, $t'(x)$, and $t''(x)$ are renormalized by the Gutzwiller factors as in the original work.[37] Energies are measured in units of the bare nearest neighbor hopping $t_0 \sim 300-400$ meV.

Pseudogap correlations enter into the self-energy $\Sigma_R(\mathbf{k},\omega) = \Delta_R(\mathbf{k})^2/(\omega + \epsilon_{0\mathbf{k}})$ which diverges at zero frequency at the umklapp surface $|k_x \pm k_y| = \pi$. Here, $\Delta_R(\mathbf{k}) = [\Delta_R(x)/2](\cos k_x - \cos k_y)$. $\Delta_R(x)$ decreases with doping x and vanishes at a topological quantum critical point x_c, as shown in Fig. 1(a). The coherent part of the YRZ Green's function is similar to the BCS diagonal one with the nontrivial difference, which in BCS, the self-energy diverges at the Fermi surface (FS) and in YRZ, it diverges at the umklapp one. There is no off-diagonal component of the Green's function in the YRZ model, and Δ_R does not break any symmetry. A crucial point in this model is the appearance of hole pockets close to $(\pm\pi/2, \pm\pi/2)$. Due to reduced spectral weight on the outer edge of the pocket, a gapless Fermi arc appears in ARPES at zero energy.[2,37] At finite binding energy, the arc structure remains, as shown in Fig. 1(c). At the critical doping x_c where $\Delta_R(x)$ vanishes, a complete FS is recovered.[37]

Superconductivity is introduced in the standard way as in Ref. 37. The diagonal Green's function becomes

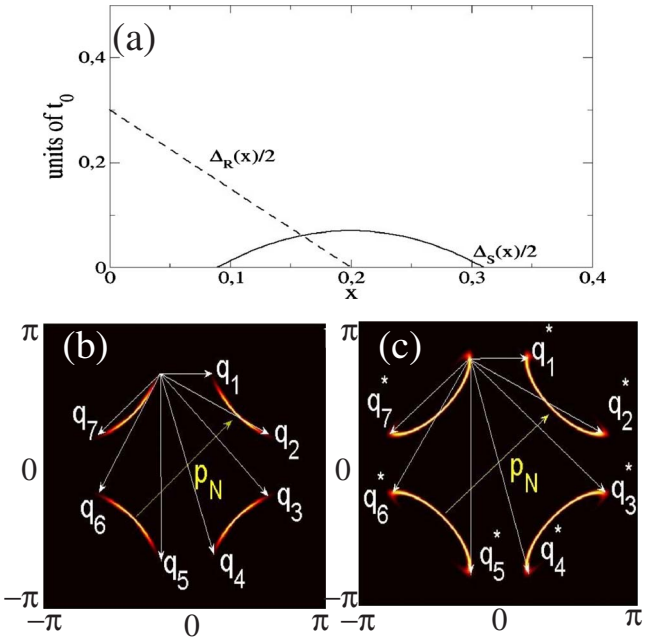

FIG. 1. (Color online) (a) Evolution of $\Delta_R(x)$ (dashed) and $\Delta_S(x)$ (solid) with doping using the same parameters as in Ref. 37. (b) ARPES intensity around the nodes in the superconducting state for $x=0.20$ and $\omega=-0.04$ in units of the bare nearest neighbor hopping. (c) Same as in (b) in the pseudogap state for $x=0.16$ according to the model discussed. The wave vectors $\mathbf{q}_i$ ($\mathbf{q}_i^*$) of quasiparticle interference patterns in the octet model, as well as the intranodal momenta along the diagonal $\mathbf{P}_N$ are shown (see text).

$$G_{SC}^{YRZ}(\mathbf{k},\omega) = \frac{g_t}{\omega - \xi(\mathbf{k}) - \Sigma_R(\mathbf{k},\omega) - \Sigma_S(\mathbf{k},\omega)}. \tag{3}$$

Here, $\Sigma_S(\mathbf{k},\omega) = |\Delta_S^2(\mathbf{k})|/]\omega + \xi(\mathbf{k}) + \Sigma_R(\mathbf{k},-\omega)]$ is the superconducting self-energy. The superconducting order parameter Δ_S is related to the critical temperature T_c and has d-wave symmetry $\Delta_S(\mathbf{k}) = [\Delta_S(x)/2](\cos k_x - \cos k_y)$. The dependence of $\Delta_S(x)$ with doping used is shown in Fig. 1(a). It is assumed that pseudogap and superconductivity coexist below T_c and x_c. Below x_c, we characterize the PG state by zero Δ_S and finite Δ_R. Beyond x_c, Δ_R vanishes and BCS behavior is recovered. The anomalous behavior, i.e., the emergence of nondispersive features, is expected below $x_c = 0.2$.

The exact expressions for the spectral function and energies of the YRZ model[2,37] $A(\mathbf{k},\omega) = -2\,\mathrm{Im}\,G(\mathbf{k},\omega)$ and $B(\mathbf{k},\omega) = -2\,\mathrm{Im}\,F(\mathbf{k},\omega)$, with $F(\mathbf{k},\omega)$, the superconducting anomalous Green's functions are

$$\begin{aligned} A(\mathbf{k},\omega) &= g_t\pi\{(v_{\mathbf{k}}^-)^2\delta(\omega + E_{\mathbf{k}}^-) + (u_{\mathbf{k}}^-)^2\delta(\omega - E_{\mathbf{k}}^-) \\ &\quad + (v_{\mathbf{k}}^+)^2\delta(\omega + E_{\mathbf{k}}^+) + (u_{\mathbf{k}}^+)^2\delta(\omega - E_{\mathbf{k}}^+)\}, \\ B(\mathbf{k},\omega) &= g_t\pi\{u_{\mathbf{k}}^- v_{\mathbf{k}}^-[\delta(\omega + E_{\mathbf{k}}^-) + \delta(\omega - E_{\mathbf{k}}^-)] \\ &\quad + u_{\mathbf{k}}^+ v_{\mathbf{k}}^+[\delta(\omega + E_{\mathbf{k}}^+) + \delta(\omega - E_{\mathbf{k}}^+)]\}, \end{aligned} \tag{4}$$

with coherence factors $v_{\mathbf{k}}^{2\pm} = \frac{1}{2}(a_{\mathbf{k}}^{\pm} - b_{\mathbf{k}}^{\pm}/E_{\mathbf{k}}^{\pm})$ and $u_{\mathbf{k}}^{2\pm} = \frac{1}{2}(a_{\mathbf{k}}^{\pm} + b_{\mathbf{k}}^{\pm}/E_{\mathbf{k}}^{\pm})$, where $a_{\mathbf{k}}^{\pm} = \frac{1}{2}[1 \pm (\xi_{\mathbf{k}}^2 - \xi_{\mathbf{k}0}^2 + \Delta_{S\mathbf{k}}^2)/E_{\mathbf{k}}^{SC}]$ and $b_{\mathbf{k}}^{\pm} = \xi_{\mathbf{k}} a_{\mathbf{k}}^{\pm} \pm \Delta_{R\mathbf{k}}^2(\xi_{\mathbf{k}} - \xi_{\mathbf{k}0})$, and energies

$$(E_{\mathbf{k}}^{\pm})^2 = \Delta_{R\mathbf{k}}^2 + \frac{\xi_{\mathbf{k}}^2 + \xi_{0\mathbf{k}}^2 + \Delta_{S\mathbf{k}}^2}{2} \pm (E_{\mathbf{k}}^{SC})^2,$$

$$(E_{\mathbf{k}}^{SC})^2 = \sqrt{(\xi_{\mathbf{k}}^2 - \xi_{0\mathbf{k}}^2 + \Delta_{S\mathbf{k}}^2)^2 + 4\Delta_{R\mathbf{k}}^2[(\xi_{\mathbf{k}} - \xi_{0\mathbf{k}})^2 + \Delta_{S\mathbf{k}}^2]}.$$

Only $A(\mathbf{k},\omega)$ enters in the AC-ARPES spectrum. To compare with experiments, we calculate Eq. (1) following the same procedure as in Refs. 35 and 36. Only those momenta $\mathbf{k}$ which satisfy that both $\mathbf{k}$ and $\mathbf{k}+\mathbf{q}$ belong to the first Brillouin zone are included in the sum. Umklapp terms do not enter and the autocorrelated spectrum does not have the lattice symmetry. To mimic finite energy resolution in ARPES, the spectral function is convoluted with a Gaussian of width $0.02t_0$. Experimental AC-ARPES spectrum is also influenced by the anisotropic and energy dependent lifetime not included here. All the calculations are performed at zero temperature as the YRZ model has been developed only in this limit.

III. RESULTS

In the so-called octet model[19] proposed to explain the FT-STS spectrum in the SC state, the largest JDOS at a given ω is found at the tips of the banana-shaped constant energy contours around the nodes and $n(\mathbf{q},\omega)$ peaks at the wavevectors $\mathbf{q}_1,\ldots,\mathbf{q}_7$ which connect such tips [see Fig. 1(b)]. The size of these banana-shape constant energy contours changes with binding energy producing the dispersive behavior of the peaks. The peaks corresponding to $\mathbf{q}_i$-type terms are observed in Fig. 2(a) where the AC-ARPES map in the SC state at $\omega=-0.04$ is shown for $x_c=0.20$, doping at which Δ_R vanishes. This map closely resembles the one obtained experimentally[35,36] in the SC state, as well as those arising from the convolution of the Green function with itself discussed in the context of FT-STS experiments,[19,20] but it lacks the kaleidoscopic patterns due to umklapp[20] present in the latest ones.

A good way to quantify the dispersion of the peaks is to look at the spectrum in a given direction at several energies. The change of momenta with binding energy of the peaks along the bond and diagonal directions is clearly seen in Figs. 2(d) and 2(g). Forgetting about zero momenta, notice that in Fig. 2(d), there is a single peak at zero frequency which splits with frequency. As the Fermi surface is completely gapped at $\omega=0$, both momenta $\mathbf{q}_1$ and $\mathbf{q}_5$ are equal and connect the nodes. The almost dispersionless peak $\mathbf{P}_N$ in Fig. 2(g) is not included in the octet model. It is due to nesting[20] and has been also seen by McElroy *et al.*[35]

The AC-ARPES map in the PG state is shown in Fig. 2(b). At first sight, the ARPES intensities in the $x \geqslant x_c$ BCS superconducting [Fig. 1(b)] and the $x < x_c$ PG states [Fig. 1(c)] look similar. However, their AC-ARPES spectrum and energy dependence show important differences. Contrary to what happens in the SC case, the peak along the bond in the AC-ARPES spectrum in the PG state is split in Fig. 2(e), *even at zero energy*. The positions of the emergent peaks change very little with energy in strong contrast to the dispersive behavior in Fig. 2(d). This weak dispersion could be further reduced by finite lifetimes, weaker spectral weight at the antinode, or worse experimental resolution than included here. Zero-energy splitting and nondispersive behavior also appear along the diagonal [Fig. 2(h)]. The peak momentum and energy dependence in Fig. 2(e) resemble that found in the PG by Chatterjee *et al.*[36] It has been shown[36] that the experimental spectrum is robust to truncation of the ARPES intensity plots to include only the Fermi arcs, what suggest the peaks correspond to vectors connecting the ends of the Fermi arcs. The small and large momentum peaks along the bond are, respectively, associated with vectors of the $\mathbf{q}_1^*$ and $\mathbf{q}_5^*$ types in Fig. 1(b). The checkerboard pattern in FT-STS is presumably related to $\mathbf{q}_1^*$ peak. We note that the momentum at which the 3/4 substructure has been observed[13] is very

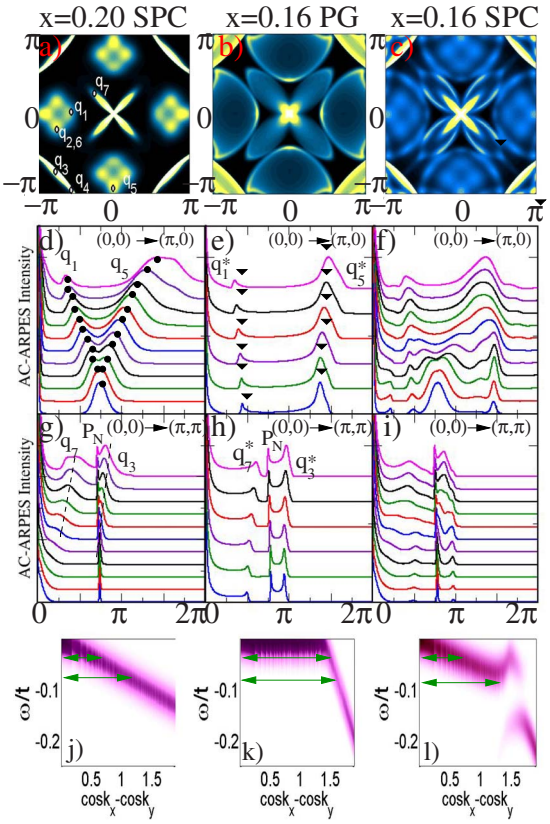

FIG. 2. (Color online) AC-ARPES and energy spectra for $x_c=0.20$ ($\Delta_R=0$, $\Delta_S=0.14$) in the superconducting state (left column) and $x_c=0.16$ in the pseudogap state ($\Delta_R=0.12$, $\Delta_S=0$, middle column) and in the superconducting state ($\Delta_R=0.12$, $\Delta_S=0.12$, right column). (a) to (c) show, in arbitrary units, the maps at $\omega=-0.04$. [(d)–(f) and (g)–(i)] Intensity of the autocorrelated spectral function along the $(0,0)-(\pi,0)$ (bond) and $(0,0)-(\pi,\pi)$ (diagonal) directions, respectively, at several energies. From bottom to top, $\omega=-0$ to -0.10 in 0.02 intervals in the pseudogap state and in 0.01 intervals in the superconducting state and in units of the bare nearest neighbor hopping. In the units chosen, $\omega \sim 3-4$ meV and the curves shown extend up to 30–40 meV. Each curve in (d) to (i) is normalized to the value at its largest feature other than the one at (0,0) and displaced to better show the peak dispersion. The different behaviors of the energy dispersion in the SC, PG, and SC and PG states can be seen in (j) to (l) where the energy spectrum along the $\omega=0$ maximum ARPES intensity line is plotted. Arrows are at $\omega=-0.04$ and $\omega=-0.08$.

close to that of the $\mathbf{q}_5^*$ peak, and we postulate that both features are related.

The origin of the different behaviors of peak position in the SC and PG states is related to the dependence of the constant-energy contour size with binding energy which can be inferred from Fig. 2(j) and 2(k), where the corresponding energy spectrum along the $\omega=0$ maximum ARPES intensity line is reproduced. The length of the arrows at $\omega=-0.04$ and $\omega=-0.08$ gives an idea on the change of the constant energy contours with binding energy. In the SC state, the zero energy contour is a single point since all the FS is gapped. The contour size increases rapidly with binding energy producing the splitting of the $\mathbf{q}_1-\mathbf{q}_5$ peak in Fig. 2(d). On the other hand, in the PG state, the peak splitting at zero energy along the bond comes from the finite size of the closed pocket centered around $(\pi/2,\pi/2)$. The size of the constant-energy contour barely changes with binding energy resulting in nondispersive behavior.

The AC-ARPES spectrum in the SC state for $x<x_c$ is shown in Figs. 2(c), 2(f), and 2(i). Interestingly, both dispersive and nondispersive features can be distinguished in Fig. 2(f). Dispersive peaks, of the type observed in Fig. 2(d), dominate at low energy, but there is a clear kink in the dispersion and the peaks in the AC-ARPES spectrum converge to those observed in the PG state. The opening of a gap due to superconductivity in the arcs suppresses the nondispersive peaks at low energies arising from the tips of the arcs, but remanent structure is visible at the corresponding momenta. The presence of both types of peaks is due to the coexistence of SC and PG. This coexistence can be seen in the energy band spectrum in Fig. 2(l) in the form of a U-shaped gap.[2,4,5,7] The gap in the arc at low energies is dominated by superconductivity. At higher energies, the spectrum in the antinodal region is influenced by both superconductivity and PG, mostly by the later one.

The dispersive and nondispersive features are better seen in Fig. 3(a), where the position of the maxima is plotted. The energy at which the change from dispersive to nondispersive behavior happens is mainly given by $\Delta_S(\mathbf{k})$ at the arc tip, and depends on Δ_R, via the arc length. Overlap of dispersive and nondispersive peaks does not always allow us to differentiate them or to associate the position of the maximum in intensity to a particular kind of peak. A change from dispersive behavior at low energies to nondispersive behavior at higher energies in the AC-ARPES of Bi2212 in the SC state has been recently reported.[38,39]

The AC-ARPES spectra, corresponding to $x=0.12$ and $x=0.18$, in the SC state along the bond are shown in Figs. 3(b) and 3(c). Here, Δ_S and Δ_R are finite in both cases. However, dispersive and nondispersive peaks are not as clearly identified here as they were in Fig. 2(e). Thus, the presence of only dispersive (nondispersive) peaks does not guarantee zero Δ_R (Δ_S). In general, for smaller $\frac{\Delta_S}{\Delta_R}$, the nondispersive structure is more pronounced, and for a given doping, the range of energies at which dispersive features appear is reduced with decreasing Δ_S. In agreement with recent ARPES measurements,[7] we expect Δ_S to be, to some extent, related to T_c. In low T_c cuprates, Δ_R and Δ_S are expected to differ more and $\frac{\Delta_S}{\Delta_R}$ to be smaller. Based on this argument, we predict that in the SC state below T_c, the peaks in the AC-ARPES spectrum of low T_c cuprates will be mostly nondispersive, similar to the ones found in the PG state in Bi2212.[36]

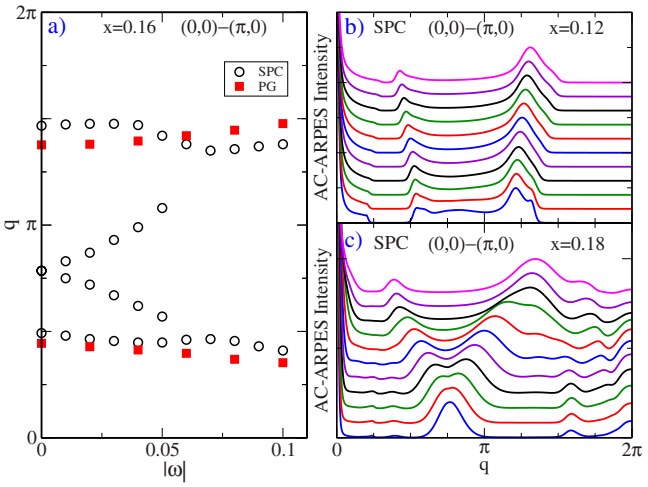

FIG. 3. (Color online) (a) Position of the dispersive and nondispersive peaks found in the $(0,0)$-$(\pi,0)$ direction in the superconducting and pseudogap state at $x=0.16$. [(b) and (c)] Same as in Fig. 2(f) but for $x=0.12$ ($\Delta_R=0.24$, $\Delta_S=0.07$) and $x=0.18$ ($\Delta_R=0.06$, $\Delta_S=0.13$), respectively.

IV. RELATION TO FOURIER TRANSFORM SCANNING TUNNELING SPECTROSCOPY EXPERIMENTS

In this paper, we have discussed the AC-ARPES spectrum. The quantities measured by AC-ARPES and FT-STS are not the same, so some discussion on the applicability of our results to FT-STS proceeds. For a more detailed discussion, see Ref. 34. Neglecting matrix element effects, in the quasiparticle interference picture, the structure in $n(\mathbf{q},\omega)$ measured by FT-STS is essentially given by the one in[19]

$$\int \frac{d^2k}{(2\pi)^2}\hat{G}_0(\mathbf{k}+\mathbf{q},\omega)T(\mathbf{k}+\mathbf{q},\mathbf{k};\omega)\hat{G}_0(\mathbf{k},\omega). \tag{5}$$

Here $\hat{G}_0$ is a 2×2 matrix which includes both the diagonal and anomalous parts, the subscript 0 means the absence of scattering and $T(\mathbf{k}+\mathbf{q},\mathbf{k};\omega)$ is the scattering matrix. The right expression for the T matrix is not evident due to the uncertainty in the proper disorder model for these materials. The most simple model assumes that the peaks in $n(\mathbf{q},\omega)$ coincide with those of

$$\int \frac{d^2k}{(2\pi)^2}\hat{G}_0(\mathbf{k}+\mathbf{q},\omega)\hat{G}_0(\mathbf{k},\omega), \tag{6}$$

i.e., that the scattering matrix does not introduce extra peaks or cancels the ones in Eq. (6). At a given energy, this integral is expected to be dominated by those $\mathbf{k}$ which satisfy the simultaneous pole equations for both Green functions[19] and to peak at those momenta $\mathbf{q}$ with the largest joint density of states. In a d-wave BCS state, this approximation results in

the octet model discussed above. The position and dispersion of the peaks predicted by the JDOS work quite well in the superconducting state. It remains to be understood why it gives the correct picture without including the T matrix.[20]

Equation (6) still differs from Eq. (1) in the presence of the anomalous spectral function $B(\mathbf{q},\omega)$ in Eq. (6) and its absence in Eq. (1). This term can modify the relative intensity of the FT-STS peaks and their energy dependence, but it does not change the pole conditions. As a result, within the JDOS picture, at a given energy, the FT-STS and AC-ARPES spectra show peaks at the same momenta $\mathbf{q}$, and our conclusion on the dispersive or nondispersive behavior can be extended to the tunneling experiments. Due to the uncertainty on the proper scattering matrix $T(\mathbf{k}+\mathbf{q},\mathbf{k};\omega)$, a direct analysis of the FT-STS spectrum most probably would not seed much more information. The similarity in the peak position found experimentally in AC-ARPES and FT-STS suggests that the JDOS applies. We do not know of any argument which could justify the appearance of peaks at the same position in the AC-ARPES and FT-STS spectrum assuming an intrinsic (not disorder induced) charge-ordering origin of the checkerboard. On the other hand, the behavior found in FT-STS agrees with our expectations.

Initially,[9] it was reported that $\lambda=4$, and the effect described as a *four*-unit cell pattern. However, it is now clear that λ varies between 4 and 5 depending on the sample. Recent experiments suggest that λ depends systematically on doping.[40] In our model, the arc length increases with doping[2,37] and $\mathbf{q}_1^*$ decreases.

In FT-STS experiments in the SC state, the checkerboard pattern is better seen in cuprates with low T_c and when the integrated density of states lacks the coherence peaks, when it is more PG-like.[13,14,16,17] Dispersive peaks were not seen in early measurements[13] in underdoped $Ca_{2-x}Na_xCuO_2Cl_2$ (Na-CCOC) with very low T_c. Very recent experiments have succeed[41] in observing dispersive behavior in nearly optimally doped Na-CCOC and found that it is restricted to low energies. Some evidence of dispersive peaks at low energies and nondispersive ones at higher energies had been reported in FT-STS experiments in underdoped Bi2212.[14] Recent experiments have confirmed the evolution of dispersive to nondispersive behavior[42] in the FT-STS spectrum of lightly doped $Bi_2Sr_2Dy_{0.2}Ca_{0.8}Cu_2O_{8+\delta}$.

V. CONCLUSIONS

In conclusion, we have shown that the nondispersive peaks found in the autocorrelation of photoemission data in Bi2212 in the pseudogap state can be explained without involving intrinsic charge ordering or symmetry breaking but the existence of the Fermi arcs and a weak binding energy dependence of the size of the constant energy contour. We believe that the nondispersive structure in FT-STS, including the weaker 3/4 substructure, can be explained within a joint density of states picture. Furthermore, we obtain the simultaneous appearance of both dispersing and nondispersing peaks in the AC-ARPES spectrum in the superconducting state of underdoped cuprates, which originates in the U shape of the SC gap and will be better observed in materials with low T_c. The presence of both dispersive and nondispersive peaks in AC-ARPES in the SC state recently reported,[38,39] and the new FT-STS[41,42] results give further support to the existence of pseudogap correlations in the superconducting state and to a common origin of the peaks observed in AC-ARPES and FT-STS.

Recent ARPES experiments[43] have suggested that in the PG state, the Fermi length is temperature dependent and vanishes at low temperatures. The observation by Chatterjee *et al.*[36] that the nondispersive peaks found in the AC-ARPES in the PG state arise from the tips of the Fermi arcs and that a SC-type gap in the arcs results in dispersive features opens a new way to get complementary information on the length of the Fermi arc. We propose that AC-ARPES experiments can be used to determine the position of the arc tips and nodal Fermi momentum, as well as of the arc length and its dependence with temperature and doping. The position of the arc tips and Fermi momenta can be determined from the $\mathbf{q}_i^*$ and $\mathbf{P}_N$ momenta at which the AC-ARPES spectrum peaks along the bond and diagonal direction. As shown experimentally,[36] these peaks are clearly resolved even in the pseudogap state. The dependence of the arc size with energy can also be measured, providing extra information of the physics involved in the truncation of the Fermi surface. We believe that low T_c cuprates are the most suitable for this experiment as the two energy scales Δ_R and Δ_S will be most different and underdoped non-SC samples, showing the checkerboard, are available.[13]

ACKNOWLEDGMENTS

We acknowledge funding from MEC through Grant No. FIS2005-05478-C02-01, Ramon y Cajal contract, from Consejería de Educación de la Comunidad de Madrid, and CSIC through Grant No. 200550M136 and an I3P contract.

*leni@icmm.csic.es

†belenv@icmm.csic.es

[1] M. R. Norman, H. Ding, M. Randeria, J. C. Campuzano, T. Yokoya, T. Takeuchi, T. Takahashi, T. Mochiku, K. Kadowaki, P. Guptasarma, and D. G. Hinks, Nature (London) **392**, 157 (1998).

[2] B. Valenzuela and E. Bascones, Phys. Rev. Lett. **98**, 227002 (2007).

[3] M. Le Tacon, A. Sacuto, A. Georges, G. Kotliar, Y. Gallais, D. Colson, and A. Forget, Nat. Phys. **2**, 138 (2006).

[4] J. Mesot, M. R. Norman, H. Ding, M. Randeria, J. C. Campuzano, A. Paramekanti, H. M. Fretwell, A. Kaminski, T. Takeuchi, T. Yokoya, T. Sato, T. Takahashi, T. Mochiku, and K. Kadowaki, Phys. Rev. Lett. **83**, 840 (1999).

[5] K. Tanaka, W. S. Lee, D. H. Lu, A. Fujimori, T. Fujii, Risdiana, I. Terasaki, D. J. Scalapino, T. P. Devereaux, Z. Hussain, and Z.-X. Shen, Science **314**, 1910 (2006).
[6] M. Hashimoto, T. Yoshida, K. Tanaka, A. Fujimori, M. Okusawa, S. Wakimoto, K. Yamada, T. Kakeshita, H. Eisaki, and S. Uchida, Phys. Rev. B **75**, 140503(R) (2007).
[7] T. Kondo, T. Takeuchi, A. Kaminski, S. Tsuda, and S. Shin, Phys. Rev. Lett. **98**, 267004 (2007).
[8] S. Chakravarty, R. B. Laughlin, D. K. Morr, and C. Nayak, Phys. Rev. B **63**, 094503 (2001); C. M. Varma, Phys. Rev. Lett. **83**, 3538 (1999); S. A. Kivelson, I. P. Bindloss, E. Fradkin, V. Oganesyan, J. M. Tranquada, A. Kapitulnik, and C. Howald, Rev. Mod. Phys. **75**, 1201 (2003).
[9] J. E. Hoffman, E. W. Hudson, K. M. Lang, V. Madhavan, H. Eisaki, S. Uchida, and J. C. Davis, Science **295**, 466 (2002).
[10] J. E. Hoffman, K. McElroy, D.-H. Lee, K. M. Lang, H. Eisaki, S. Uchida, and J. C. Davis, Science **297**, 1148 (2002).
[11] K. McElroy, R. W. Simmonds, J. E. Hoffman, D. H. Lee, J. Orenstein, H. Eisaki, S. Uchida, and J. C. Davis, Nature (London) **422**, 592 (2003).
[12] M. Vershinin, S. Misra, S. Ono, Y. Abe, Y. Ando, and A. Yazdani, Science **303**, 1995 (2004).
[13] T. Hanaguri, C. Lupien, Y. Kohsaka, D. -H. Lee, M. Azuma, M. Takano, H. Takagi, and J. C. Davis, Nature (London) **430**, 1001 (2004).
[14] K. McElroy, D. H. Lee, J. E. Hoffman, K. M. Lang, J. Lee, E. W. Hudson, H. Eisaki, S. Uchida, and J. C. Davis, Phys. Rev. Lett. **94**, 197005 (2005).
[15] G. Levy, M. Kugler, A. A. Manuel, O. Fischer, and M. Li, Phys. Rev. Lett. **95**, 257005 (2005).
[16] A. Hashimoto, N. Momono, M. Oda, and M. Ido, Phys. Rev. B **74**, 064508 (2006).
[17] T. Machida, Y. Kamijo, K. Harada, T. Noguchi, R. Saito, T. Kato, and H. Sakata, J. Phys. Soc. Jpn. **75**, 083708 (2006).
[18] C. Howald, H. Eisaki, N. Kaneko, M. Greven, and A. Kapitulnik, Phys. Rev. B **67**, 014533 (2003).
[19] Q.-H. Wang and D.-H. Lee, Phys. Rev. B **67**, 020511(R) (2003).
[20] L. Capriotti, D. J. Scalapino, and R. D. Sedgewick, Phys. Rev. B **68**, 014508 (2003); T. Pereg-Barnea and M. Franz, Phys. Rev. B **68**, 180506(R) (2003).
[21] L. Zhu, W. A. Atkinson, and P. J. Hirschfeld, Phys. Rev. B **69**, 060503(R) (2004); T. S. Nunner, W. Chen, B. M. Andersen, A. Melikyan, and P. J. Hirschfeld, *ibid.* **73**, 104511 (2006).
[22] S. Misra, M. Vershinin, P. Phillips, and A. Yazdani, Phys. Rev. B **70**, 220503(R) (2004).
[23] C. Bena, S. Chakravarty, J. Hu, and C. Nayak, Phys. Rev. B **69**, 134517 (2004); A. Ghosal, A. Kopp, and S. Chakravarty, *ibid.* **72**, 220502(R) (2005).
[24] H.-D. Chen, J.-P. Hu, S. Capponi, E. Arrigoni, and S.-C. Zhang, Phys. Rev. Lett. **89**, 137004 (2002).
[25] Z. Tesanovic, Phys. Rev. Lett. **93**, 217004 (2004).
[26] A. Polkovnikov, M. Vojta, and S. Sachdev, Phys. Rev. B **65**, 220509(R) (2002).
[27] D. Podolsky, E. Demler, K. Damle, and B. I. Halperin, Phys. Rev. B **67**, 094514 (2003).
[28] M. Vojta, Phys. Rev. B **66**, 104505 (2002).
[29] P. W. Anderson, arXiv:cond-mat/0406038 (unpublished).
[30] F. J. Ohkawa, Phys. Rev. B **73**, 092506 (2006).
[31] C. Li, S. Zhou, and Z. Wang, Phys. Rev. B **73**, 060501(R) (2006).
[32] J.-X. Li, C.-Q. Wu, and D.-H. Lee, Phys. Rev. B **74**, 184515 (2006).
[33] L. Dell'Anna, J. Lorenzana, M. Capone, C. Castellani, and M. Grilli, Phys. Rev. B **71**, 064518 (2005).
[34] R. S. Markiewicz, Phys. Rev. B **69**, 214517 (2004).
[35] K. McElroy, G.-H. Gweon, S. Y. Zhou, J. Graf, S. Uchida, H. Eisaki, H. Takagi, T. Sasagawa, D.-H. Lee, and A. Lanzara, Phys. Rev. Lett. **96**, 067005 (2006).
[36] U. Chatterjee, M. Shi, A. Kaminski, A. Kanigel, H. M. Fretwell, K. Terashima, T. Takahashi, S. Rosenkranz, Z. Z. Li, H. Raffy, A. Santander-Syro, K. Kadowaki, M. R. Norman, M. Randeria, and J. C. Campuzano, Phys. Rev. Lett. **96**, 107006 (2006).
[37] K.-Y. Yang, T. M. Rice, and F.-C. Zhang, Phys. Rev. B **73**, 174501 (2006).
[38] U. Chatterjee, M. Shi, A. Kaminski, A. Kanigel, H. M. Fretwell, K. Terashima, T. Takahashi, S. Rosenkranz, Z. Z. Li, H. Raffy, A. Santander-Syro, K. Kadowaki, M. Randeria, M. R. Norman, and J. C. Campuzano, Phys. Rev. B **76**, 012504 (2007).
[39] E. Bascones and B. Valenzuela, arXiv:cond-mat/0702111 (unpublished). This prediction was already included in the first version of this paper.
[40] J. C. Seamus Davis (private communication).
[41] T. Hanaguri, Y. Kohsaka, J. C. Davis, C. Lupien, I. Yamada, M. Azuma, M. Takano, K. Ohishi, M. Ono, and H. Takagi, Nat. Phys. **3**, 865 (2007).
[42] J. C. Seamus Davis, Talk at the Yamada Conference XI: Spectroscopies in Novel Superconductors, Sendai, August 2007 (unpublished).
[43] A. Kanigel, M. R. Norman, M. Randeria, U. Chatterjee, S. Suoma, A. Kaminski, H. M. Fretwell, S. Rosenkranz, M. Shi, T. Sato, T. Takahashi, Z. Z. Li, H. Raffy, K. Kadowaki, D. Hinks, L. Ozyuzer, and J. C. Campuzano, Nat. Phys. **2**, 447 (2006).